Energy variation of earthquake ground motion in time frequency domain using Wavelet Transform

T. Hirai[1] and S. Sawada[2]

[1] *NEWJEC Inc., Japan*
[2] *Professor, Disaster Prevention Research Institute Kyoto Univ., Japan*
Email: hiraits@newjec.co.jp, sawada@catfish.dpri.kyoto-u.ac.jp

ABSTRACT :

The characteristics of seismic wave energy are examined in this study. The attenuation equation of total seismic wave energy with respect to moment magnitude and hypocentral distance is proposed in order to estimate the seismic intensity. It is concluded that the total seismic wave energy should be better than PGA to estimate seismic motion with respect to earthquake magnitude stably. We also show the time – frequency characteristic of the seismic wave energy of the non-stationary earthquake ground motions based on wavelet transform using Meyer wavelet. It is found that the frequency distribution of seismic wave energy can be mainly explained by the omega-square source model.

KEYWORDS: Seismic wave energy, Wavelet transform, Attenuation equation

1. INTRODUCTION

Recently the design earthquake ground motions for important infrastructures are often evaluated on the basis of numerical simulation such as the stochastic and empirical Green's function methods [1]. At that time it is necessary to show the validity of the design motion because a large uncertainty exists in setting of parameters representing the source, path and local site effects. For the purpose mentioned above, the variations in observed earthquake ground motion should be discussed. Many researchers have proposed attenuation equations to evaluate peak values such as PGA, PGV and so on [2,3,4]. It is obvious, however, that these peak values should not be enough to represent the characteristics of earthquake ground motion. In addition, few studies have been reported to discuss the variation among sites and events. Some researches indicate that energy indexes have higher correlation with earthquake damage of geotechnical works such as harbor structures than PGA and PGV [5]. In this study, we adopt total seismic wave energy as an index of strong ground motion. We propose the attenuation equation of seismic energy and examine the time – frequency characteristic of the energy of the non-stationary earthquake ground motions based on wavelet transform.

2. ATTENUATION EQUATION OF SEISMIC WAVE ENERGY

2.1. Definition of seismic wave energy

There are several studies for the seismic wave energy [6,7,8]. We adopt the definition of total seismic wave energy passing through the unit volume as

$$E = \frac{1}{2}\rho Vs\int_0^t v(t)^2\,dt \tag{2.1}$$

where $v(t)$ is the velocity time history of incident (up-going) seismic wave (= $\sqrt{(v_x^2+v_y^2+v_z^2)}$).

2.2. Database for analysis

Design earthquake motion is often defined as a twice of incident wave in the engineering base layer. We

examine attenuation relationship of total seismic wave energy in the engineering base layer. K-NET records [9], one of the dense observation networks in Japan, are used for the analysis. Although the seismographs of K-NET are installed on ground surface, soil profiles up to 20m depths are obtained at the site. **Table 2.1** lists the records used in the analysis. We adopt the events occurring after 1997, at the depth less than 30km, with JMA magnitude greater than 5.5 and recorded at more than 10 sites. In the case many large aftershocks occurred, we choose two events, these are the main shock and largest aftershock. We calculate the waveforms in the engineering base layer from the seismic records on ground surface whose PGA are more than 10 gal, based on the equivalent linear seismic response analysis (SHAKE). Note that the engineering base layers are recognized whose S-wave velocity are more than 300m/s. The sites whose soil profiles do not include the engineering base layer are not used. Strain-dependent nonlinear characteristic of sand and clay are considered [10], while effect of earth pressure on the nonlinear characteristic is only considered for sand. In the case the maximum strain calculated in seismic response analysis is larger than 0.3%, the record is not used because it is beyond applicability of equivalent linear analysis.

Table 2.1 List of the earthquakes in the database

date				Mw	number of recordings		name
					hypocentral distance < 100km	all	
1997	3	26	17 : 31	6.1	41	59	Kagoshimaken-Hokuseibu Earthquake
1997	5	13	14 : 38	6	38	56	
1997	6	25	18 : 50	5.8	26	78	
1998	5	3	11 : 9	5.5	18	18	
1998	9	3	16 : 58	5.9	16	21	
2000	10	6	13 : 30	6.6	37	148	Tottori-ken seibu Earthquake
2003	7	26	0 : 13	5.5	26	47	
2003	7	26	7 : 13	6.1	26	82	Northern Miyagi Earthquake
2004	10	23	17 : 56	6.6	32	130	Niigata chuetu Earthquake
2004	10	23	18 : 34	6.3	29	118	
2004	12	14	14 : 56	5.7	16	21	
2005	3	20	10 : 53	6.6	31	98	Fukuokaken seiho-oki Earthquake
2006	4	21	2 : 50	5.6	27	27	
2007	3	25	9 : 42	6.7	15	73	Noto-hanto Earthquake
2007	7	16	10 : 13	6.6	23	123	Niigata-ken chuetu-oki Earthquake
2007	7	16	15 : 37	5.6	25	53	
2008	6	14	8 : 43	6.9	36	118	Iwte-miyagi nairiku Earthquake

2.3.regression analysis

We use the most basic type of attenuation equation for the regression analysis as,

$$\log(E) = aM_w - b\log(X) + c \tag{2.2}$$

where, E is total seismic wave energy on the engineering base layer(J/m^2), M_w moment magnitude, X hypocentral distance(km) and a,b,c are regression coefficients. Note that no offset is considered in the distance term because we do not use near-field records whose hypocentral distances are less than 10 km. The two-step regression analysis using dummy parameters [11] is adopted. At the first step, distance coefficient b for all earthquakes and α_i ($=aM_w+c$)for each earthquake are determined as following;

$$\log(E) = \sum \delta_{ij}\alpha_i - b\log(X) \tag{2.3}$$

where, δ_{ij} is kronecker's delta function and i the number of earthquake. Coefficients a and c are determined

by regression analysis using Eqn. 2.4 at the next step.

$$\alpha = aM_w + c \tag{2.4}$$

We obtained a=1.486, b=1.752 and c=-3.668 based on 1270 records shown by marks in **Fig. 3.1**. However, the attenuation formula estimates a little smaller than the observed value. It may be because the records whose hypocentral distances are more than 100km have larger scattering. We perform another regression analysis based on the records whose hypocentral distances are less than 100km and obtain a=1.560, b=2.307 and c=-3.136. The attenuation relationship is shown by lines in **Fig. 3.1**. The relationship is also compared with the records during the 2000 Tottori-ken-seibu and the 2008 Iwate-miyagi-nairiku earthquakes, as shown in **Figs. 3.2**. The observed values during the individual earthquakes agree well with the proposed attenuation relationship.

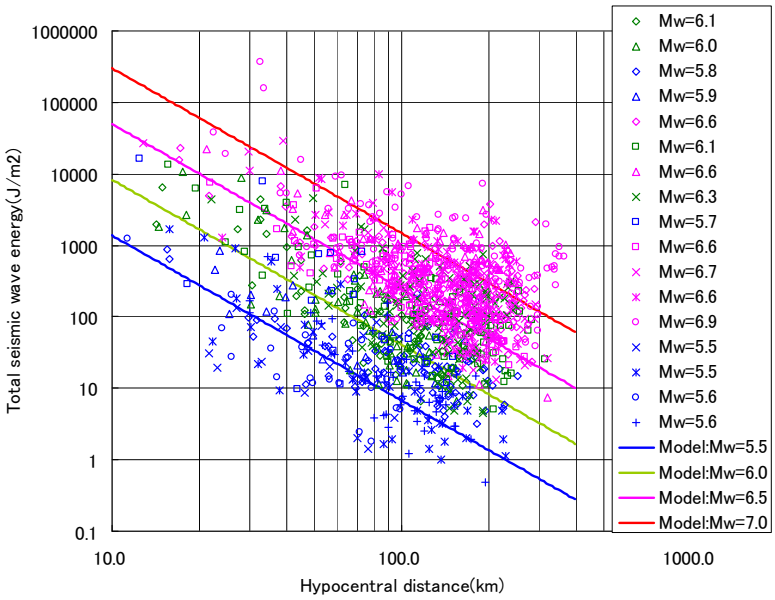

Fig. 3.1 Comparison of attenuation equation with the observed value

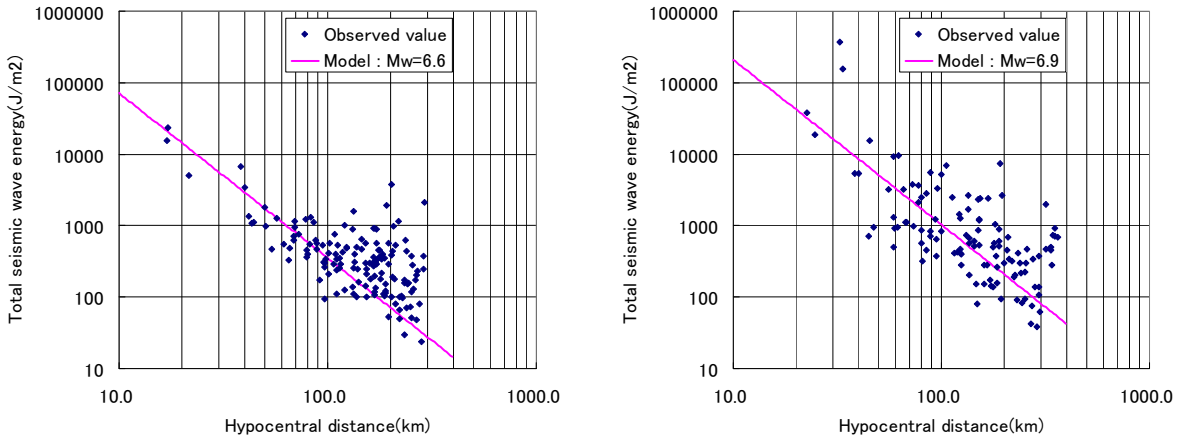

(a) Tottori-ken seibu Earthquake (b)Iwate-miyagi nairiku Earthquake

Fig. 3.2 Comparison of attenuation equation with the observed values during recent large earthquakes

We examine the difference between the sites. Site amplification characteristics are evaluated at many sites of K-NET [12]. The site amplification factors from seismic bedrock to engineering base layer of NIG008 are larger than NIG005 as shown in **Fig. 3.3**. The total seismic wave energy at NIG008 (cross marks) and NIG005 (circle marks) and corresponding attenuation relationships (lines) are shown in **Fig. 3.4**. Most of the

observed values for NIG008 are larger than the estimated values, while those for NIG005 smaller. It implies that the site amplification factor affects the seismic wave energy observed. The differences between site amplification factors may be a reason why the observed seismic wave energies have large scattering as shown in **Figs.3.1** and **3.2**.

We also examine the difference between the main and after shocks. **Fig. 3.5** shows the comparison of PGA, total seismic wave energy and hypocentral distance between the main shock (Mw=6.6) and the largest aftershock (Mw=6.3) of 2004 Niigata-chuetu earthquake. It is shown that the hypocentral distances and PGAs have little differences, while seismic wave energies of the main shock are larger than those of the after shock. The total seismic wave energy should be better than PGA to estimate seismic motion with respect to earthquake magnitude stably.

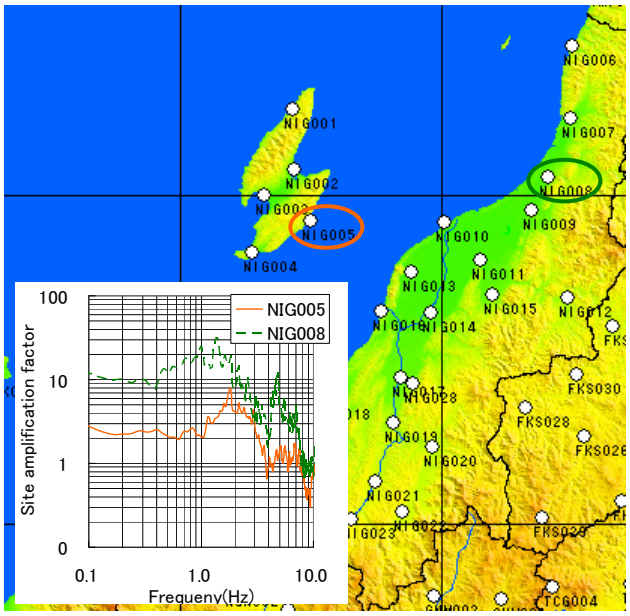

Fig. 3.3 Site amplification factor from seismic bedrock to engineering base layer

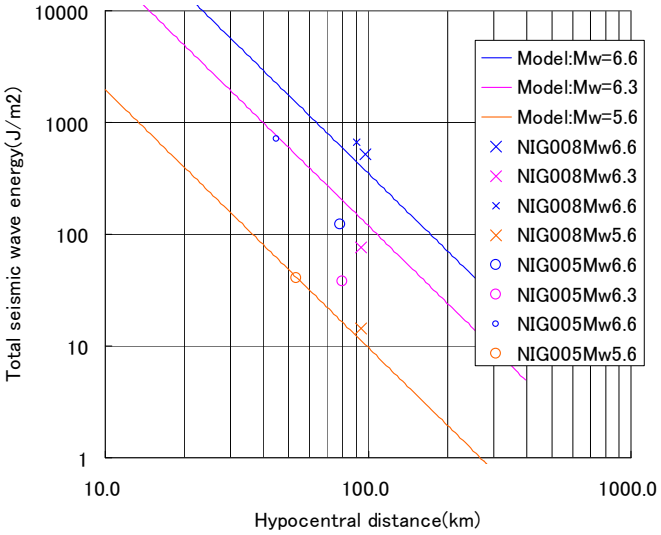

Fig. 3.4 Difference of total seismic wave energy between NIG005(circle marks) and NIG008(cross marks)

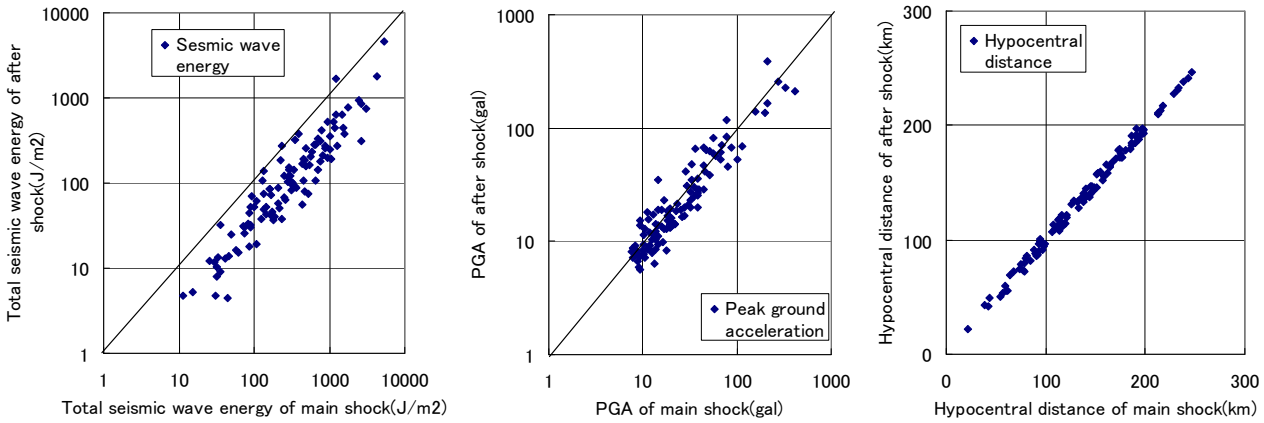

Fig. 3.5 Comparison of main shock and after shock

4. ENERGY VALIATION OF SESMIC WAVES USING WAVELET TRANSFORM

4.1.Wavelet transform

Wavelet transform is one of powerful technique for the time – frequency analysis. Its forward and inverse transformations are described as

$$T_{m,n} = \sum_m \sum_n v(t)\psi_{m,n}(t) \tag{4.1}$$

$$v(t) = \sum_m \sum_n T_{m,n}\psi_{m,n}(t) \tag{4.2}$$

$$\psi_{m,n}(t) = 2^{-m/2}\psi(2^{-m}t - n) \tag{4.3}$$

where, $\phi(t)$ is the orthogonal wavelet, $v(t)$ the input signal, $T_{m,n}$ wavelet coefficient for m-th level, m the dilation parameter, n the location parameter. Inverse transform of Discrete Wavelet Transform (DWT) is described using multi resolution representation as

$$d_m(t) = \sum_n T_{m,n}\psi_{m,n}(t) \tag{4.4}$$

$$v(t) = \sum_m d_m(t) \tag{4.5}$$

where, $d_m(t)$ is m-th resolution level of $v(t)$. The seismic wave energy of each resolution level is represented on the basis of the orthogonal characteristic of wavelet, as shown in Eqn. 4.6.

$$E = \frac{1}{2}\rho V_s \int_0^t v^2 dt = \frac{1}{2}\rho V_s \left(\int_0^t \sum_m d_m{}^2 dt + \int_0^t \sum_{m \neq n} d_m d_n dt \right) = \frac{1}{2}\rho V_s \sum_m \int_0^t d_m{}^2 dt = \frac{1}{2}\rho V_s \sum_m E_m \tag{4.6}$$

where E_m is the seismic wave energy of m-th resolution level. We adopt Mayer wavelet as the orthogonal wavelet shown in **Fig. 4.1** [13]. As Meyer wavelet is localized in frequency domain, the results of wavelet transform can be compared with those of Fourier transform [14]. An example of band-passed waveforms based on the wavelet transform and the growth of seismic wave energy of each resolution level are shown in **Fig. 4.2.** The frequency band of each resolution level used in this paper is also shown in **Table 4.1**.

4.2.Evaluation of the energy indexes

We examine the characteristics of earthquake ground motion using the following indexes;

1) Seismic wave energy of each resolution level (E_m),
2) The ratio of seismic wave energy of each resolution level with total seismic wave energy (E_m / E).

Fig. 4.3 shows distribution of the seismic wave energy for the observed ground motion and its attenuation relationship calculated by the same method described before, in each resolution level. **Fig. 4.4** shows the calculated coefficients of attenuation equation at each resolution level. The coefficient *a*, which is related to the moment magnitude, is large at the low levels as shown in **Fig.4.4(a)**. Considering the omega-square scaling model, in which Fourier amplitude of displacement wave is flat in low frequency range and decreases as frequency *f* increases with the gradient factor of f^{-2}, the difference of Fourier amplitude between large and small earthquakes is large in low frequency range and small in high frequency range, as shown in **Fig.4.5**. It implied that effect of earthquake magnitude on the seismic wave energy, that is the coefficient *a*, should be large at the low levels. On the other hand, the coefficient *b*, which is related to the hypocentral distance, is large at high levels as shown in **Fig.4.4 (b)**. As large *b* corresponds with large damping in the wave propagation path, The result in **Fig.4.4(b)** agrees with the well-known fact that the internal damping factor is large in high frequency range. **Fig.4.6** shows the contribution ratio of seismic wave energy of each resolution level with respect to the

total energy. The ratios in the low resolution levels are larger than those in higher resolution levels, while the ratios in all resolution levels have no clear relationship with the hypocentral distance. It can be explained that the frequency characteristics of seismic wave energy has close relationship with the Fourier displacement amplitude represented by the omega-square source model, in which the largest value flat in low frequency range corresponds to the seismic moment.

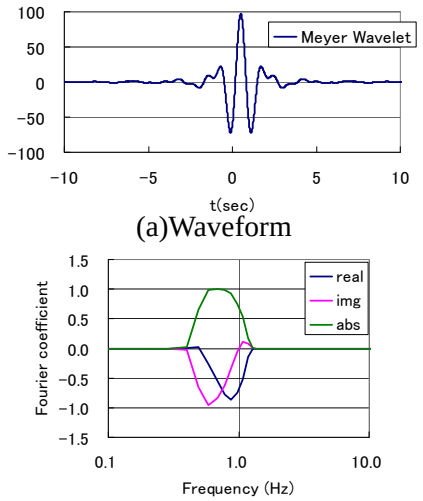

(a)Waveform

(b) Fourier spectrum

Fig. 4.1 Meyer wavelet

Table 4.1 Frequency range of each resolution level

Level	Frequency range(Hz)
0	– 0.008
1	0.004 – 0.016
2	0.008 – 0.033
3	0.016 – 0.065
4	0.033 – 0.130
5	0.065 – 0.260
6	0.130 – 0.521
7	0.260 – 1.042
8	0.521 – 2.083
9	1.042 – 4.167
10	2.083 – 8.333
11	4.167 – 16.667
12	8.333 – 33.333
13	16.667 –

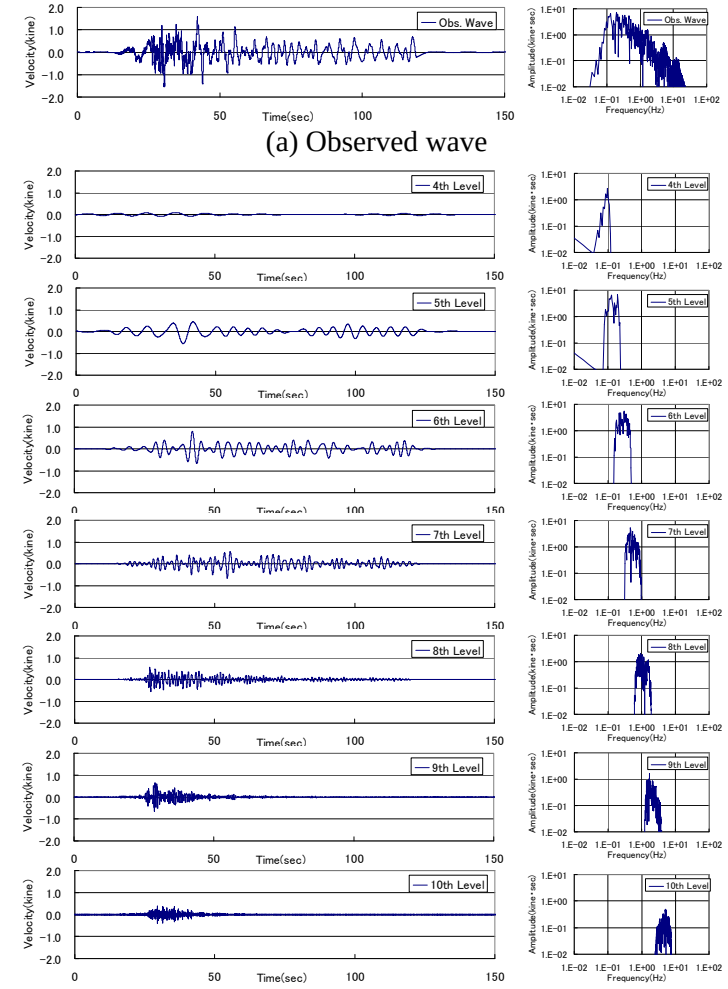

(a) Observed wave

(b) Band-passed waveform of each resolution level

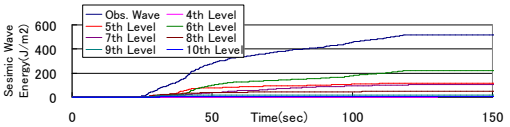

(c) Increase of seismic wave energy of each resolution level

Fig. 4.2 An example of wavelet transform

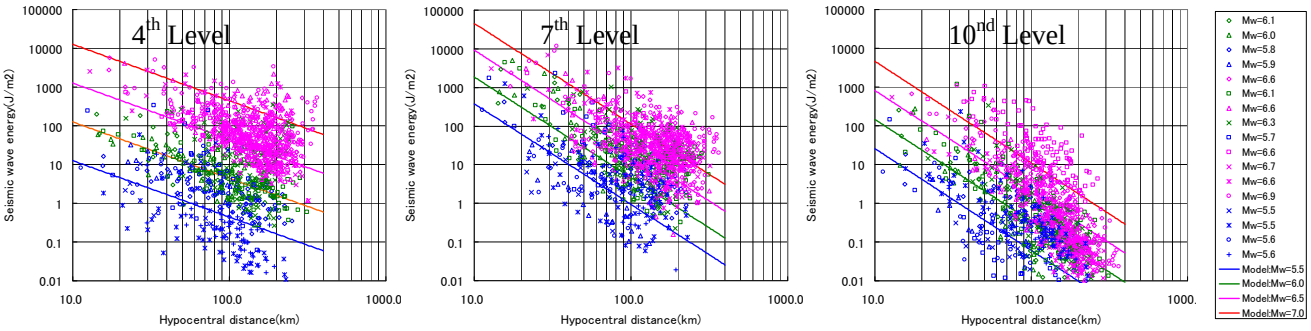

Fig. 4.3 Seismic wave energy of each resolution level

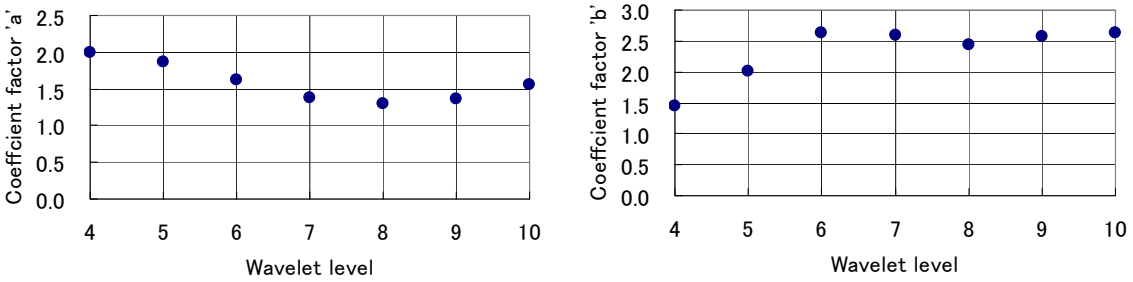

(a) Coefficient *a* (b) Coefficient *b*

Fig. 4.4 Coefficient factor of each resolution level

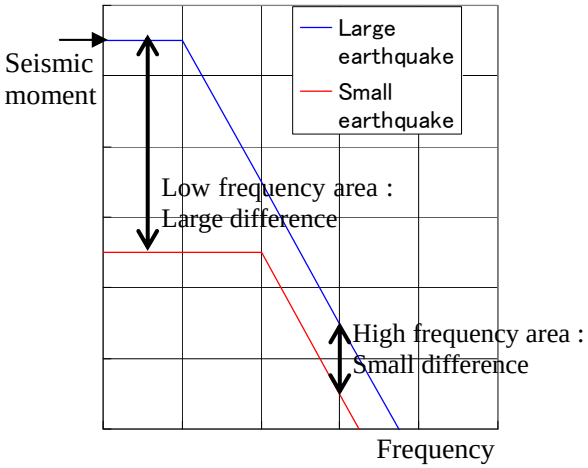

Fig. 4.5 Omega-square model

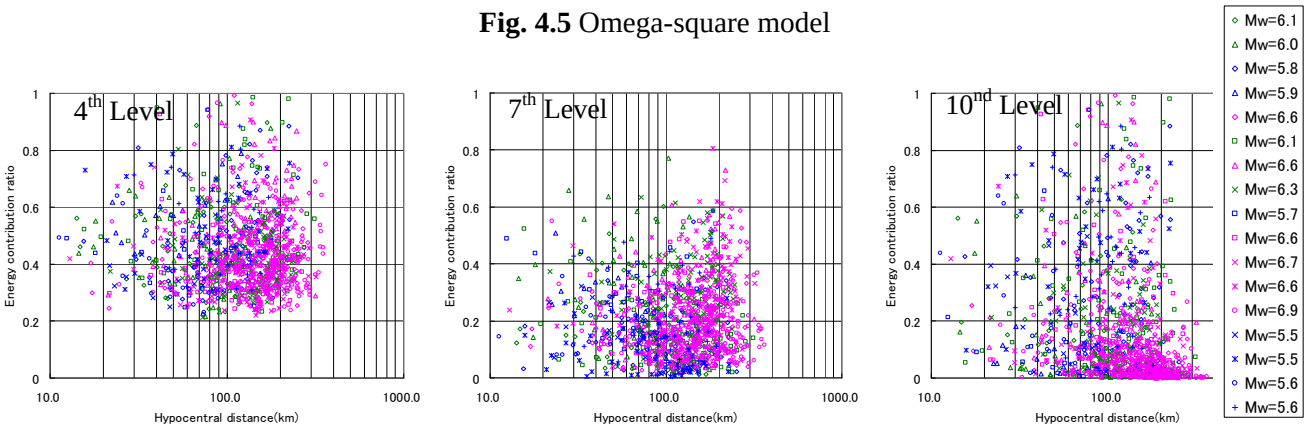

Fig. 4.6 Energy contribution ratio of each resolution level with respect to total seismic wave energy

5. CONCLUSIONS

The characteristics of seismic wave energy are examined in this study. We proposed the attenuation equation of the total seismic wave energy with respect to moment magnitude and hypocentral distance. The frequency distribution of seismic wave energy is also evaluated by the wavelet transform analysis using Meyer wavelet. We obtain the attenuation equation of the seismic wave energy at each resolution level of wavelet transform. The characteristics of seismic wave energy found in this study are as follows;

1) The seismic wave energy is a better index than PGA to estimate the seismic intensity stably and rationally.
2) The effect of earthquake magnitude on seismic wave energy is large in low frequency range.
3) The seismic wave energy in high frequency range rapidly decreases as hypocentral distance increase. It corresponds with the fact that the internal damping factor is large in high frequency range.
4) The contribution ratio of seismic wave energy of each resolution level with respect to the total energy is larger at low frequency range. It can be agreed with the omega-square source model.

REFERENCES

1 Kamae, K., and Irikura, K (1998). Source model of the Hyogo-ken Nanbu Earthquake and simulation of near-source ground motion. *Bull. Seism. Soc. Am.* **88,** 400-412.
2 Fukushima, Y. and Tanaka, T. (1988). A new attenuation relationship for peak ground accelerations derived from strong-motion accelerograms. *Proceedings of Ninth Conference of Earthquake Engineering* **II,** 343-348.
3 Si, H. and Midorikawa, S. (1999). New attenuation relationships for peak ground acceleration and velocity considering effects of fault type and site condition. *Journal of Structural and Construction Engineering* **523,** 63-70. (in Japanese)
4 Iai, S., Kurata, E. and Mukai, K. (1992). An attenuation relation for strong earthquake motions in Japan. *Technical Note of The Port and Harbour Research Institute Ministry of Transport* **724.** (in Japanese)
5 Nozu, A. and Iai, S. (2001) A study on strong motion indexes for quick damage estimation of quay wall. *Proceedings of 28th Technical meeting of Kanto Branch of Japan Society of Civil Engineers*, 18-19. (in Japanese)
6 Takagi, S (1969). Relation between the maximum value of seismic waves energy and the siesmic intensity. *Papers in Meteorology and Geophysics* **20:1,** 79-89. (in Japanese)
7 Kokusho, T., Motoyama, R., Mantani, S. and Motoyama, H. (2004). Energy flow of seismic waves in surface ground for performance-based design. *Journal of Japan Association for Earthquake Engineering* **4:4,** 1-20. (in Japanese)
8 Aki, K and Richards, P. G. (2002). Quantitative seismology second edition *Kokonshoin*. (in Japanese)
9 Kinoshita, S., Uehara, M., Tozawa, T., Wada, Y. and Ogue, Y. (1997). Recording characteristics of the K-NET95 strong-motion seismograph. *Journal of the Seismological Society of Japan* **49:4** 467-481. (in Japanese)
10 Zen, K, Yamasaki, H., and Umehara, Y. (1987). Experimental study on shear modulus and damping ratio of natural deposits for seismic response alalysis. *Repor of The Port and Harbour Research Institute* **26:1,** 41-114. (in Japanese)
11 Joyner, W. B. and Boore, D. M. (1981). Peak horizontal acceleration and velocity from strong-motion records including records from Imperial Valley. *Bull. Seism. Soc. Am.* **71,** 2011-2038.
12 Nozu, A. and Nagao, T. (2005). Site amplification factors for strong-motion sites in Japan based on spectral inversion technique. *Technical Note of The Port and Harbour Research Institute Ministry of Transport* **1112**. (in Japanese)
13 Meyer Y. (1989). Orthonormal Wavelets, in Wavelets *Springer***,** 21-37.
14 Sasaki, F., Maeda, T. and Yamada, M. (1992). Study of time history data using wavelet transform. *Journal of Structural Engineering* **38B,** 9-20. (in Japanese)